Triazole-Linked Dumbbell Oligodeoxynucleotides with NF-κB Binding Ability as Potential Decoy Molecules

ARTICLE *in* THE JOURNAL OF ORGANIC CHEMISTRY · APRIL 2008

Impact Factor: 4.72 · DOI: 10.1021/jo702459b · Source: PubMed

3 AUTHORS, INCLUDING:

Satoshi Ichikawa
Hokkaido University
101 PUBLICATIONS **1,428** CITATIONS
SEE PROFILE

Akira Matsuda
Hokkaido University
713 PUBLICATIONS **10,161** CITATIONS
SEE PROFILE

JOC Article

Triazole-Linked Dumbbell Oligodeoxynucleotides with NF-κB Binding Ability as Potential Decoy Molecules

Masanori Nakane, Satoshi Ichikawa,* and Akira Matsuda*

Faculty of Pharmaceutical Sciences, Hokkaido University, Sapporo 060-0812, Japan

matuda@pharm.hokudai.ac.jp; ichikawa@pharm.hokudai.ac.jp

Received November 16, 2007

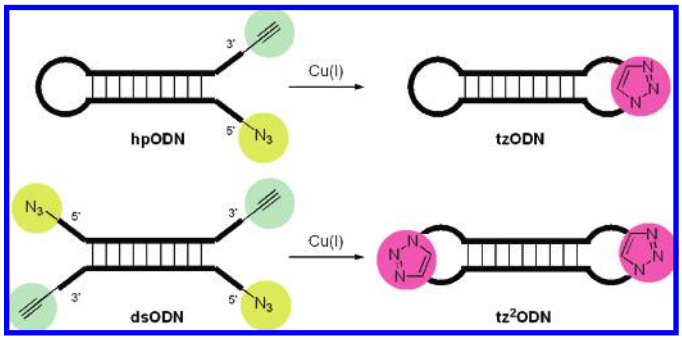

Triazole-cross-linked oligodeoxynucleotides were synthesized with use of the Cu(I) catalyzed alkyne−azide cycloaddition (CuAAC) with oligodeoxynucleotides possessing *N*-3-(azidoethyl)thymidine and *N*-3-(propargyl)thymidine at the 3′- and 5′-termini. The newly synthesized oligodeoxynucleotides were thermally stable and their global structures retained those of non-cross-linked oligodeoxynucleotides. The newly synthesized dumbbell oligodeoxynucleotides showed excellent stability against snake venom phosphodiesterase (3′-exonuclease) and high thermal stability, which are necessary for decoy molecules to achieve biological responses leading to alteration of gene expression. Moreover, dumbbell oligodeoxynucleotides have the ability to bind to NF-κB p50 homodimer within a similar range to that of a control double-stranded decoy oligodeoxynucleotide. This strategy allows us to prepare triazole-linked dumbbell oligodeoxynucleotides with a range of loop lengths, and we found that the greater the number of the thymidine residues constituting the loop region, the higher the binding affinity of the dumbbell oligodeoxynucleotides to the nuclear factor κB. This means that a protein binding ability of the dumbbell oligodeoxynucleotides could be modulated by altering the loop size. This study clearly shows that cross-linking by the triazole structure does not prevent the dumbbell oligodeoxynucleotides from binding to the nuclear factor κB transcription factor. Therefore, the results obtained conclusively demonstrate that the triazole cross-linked dumbbell oligodeoxynucleotides could be proposed as powerful decoy molecules.

Introduction

The accumulation of gene products caused by the aberrant activation and expression of the corresponding *cis*-element is involved in the initiation and progression of pathogenesis. The altered activation of transcription factors is now known to be a component of many pathways of disease pathogenesis, and the development of strategies regulating transcription factors has emerged as an attractive field of investigation.[1] Recently much effort has been dedicated to the application of the relatively short double-stranded oligodeoxynucleotides (ODNs) in developing therapeutic agents as *cis*-elements, referred to as decoy ODNs, to trap *trans*-activators, transcription factors.[2−4] Thus once delivered to cells, the decoy ODNs bearing a consensus binding sequence of a specific transcription factor are specifically recognized by the target protein. Interaction with the decoy ODNs prevents the target protein from binding to its *cis*-element. As a result, activation and expression of the corresponding *cis*-element are silenced.[5,6] The transcriptional decoy strategy against

(1) Papavassiliou, A. G. *Mol. Med. Today* **1998**, *4*, 358−366.

(2) Morishita, R.; Higaki, J.; Tomita, N.; Ogihara, T. *Circ. Res.* **1998**, *82*, 1023−1028.

(3) Cho-Chung, Y. S.; Park, Y. G.; Lee, Y. N. *Curr. Opin. Mol. Ther.* **1999**, *1*, 386−392.

(4) Mann, M. J.; Dzau, T. J. *J. Clin. Invest.* **2000**, *106*, 1071−1075.

10.1021/jo702459b CCC: $40.75
Published on Web 02/01/2008

nuclear factor κB (NF-κB) is one of the most effective approaches.[7] Activation of NF-κB upregulates genes related to inflammatory and immunological responses, such as TNF-α, adhesion molecules, macrophage colony-stimulating factor (M-CSF), granulocyte/macrophage colony-stimulating factor (GM-CSF), and monocyte chemoattractant protein (MCP). Therefore, transfection of NF-κB decoy ODNs leads to anti-inflammatory and immuno-suppressive activities.[8−15] However, several shortcomings of the decoy strategy modulating transcription factors make its practical application to biological systems unfeasible as yet. Generally, relatively short double-stranded ODNs are used in the decoy strategy and possess less thermal stability under physiological conditions. Another drawback is the presence of extra- and intracellular nucleases, which cleave ODNs.[16,17] To achieve thermal stability and resistance to nucleases, structural alteration or chemical modification of decoy ODNs is necessary.[18−26] Dumbbell ODNs, which are circular ODNs consisting of double-stranded stem region and nucleotide loops at both of their termini, possess increased exonuclease resistance because they have no terminal nucleotide residues.[27−29] Dumbbell decoy ODNs against NF-κB were shown to inhibit in vitro and ex vivo transcription. These ODNs were prepared by enzymatically ligating two identical molecules.[27,30] However, in some cases, it is difficult to provide large quantities of modified ODNs by enzymatic preparation.[31,32] An alternative approach for cross-linking nucleic acids might be chemical modification, where a chemically reactive functional group is placed site-specifically in proximity to the opposing strands of a duplex.[33] Additionally, chemical modification at both terminal positions of the double-stranded ODNs with covalent cross-linking providing dumbbell-like ODNs is expected to resist degradation catalyzed by enzymes such as exonucleases.[34] One of the strategies to cross-link double-stranded ODNs at the termini is the oxidation of thiols to form a disulfide, as reported by Glick et al.[35,36] Terminal cross-linking of double-stranded ODNs increases the thermal stability of the double-stranded ODNs and does not cause significant structural changes to the internal helix. Therefore this strategy has been used to investigate the structure of double-stranded ODNs. Though this oxidation proceeds quickly and is effective, it is reversible and the resulting disulfide bond might be easily cleaved by nucleophiles existing in the biological system. Other chemical modifications of ODNs without cross-links have also been studied including α-ODN/β-ODN duplexes,[37] phosphorothioate-modified ODNs,[16,38] PNA-DNA chimera,[39,40] and LNA-DNA chimera,[41] respectively, although they all have drawbacks.

The Hüisgen reaction is a 1,3-dipolar cycloaddition between azide and alkyne groups to afford a chemically stable 1,2,3-triazole. The usual thermal cycloaddition by heating gives both the 1,4- and 1,5-disubstituted triazoles with diminished regioselectivity; however, a long reaction time is necessary. On the other hand, the Cu(I)-catalyzed alkyne−azide cycloaddition (CuAAC),[42] which is known as "Click Chemistry",[43] proceeds quite rapidly in a variety of solvents including aqueous media

(5) Bielinska, A.; Shivdasani, R. A.; Zhang, L.; Nabel, G. J. *Science* **1990**, *250*, 997−1000.
(6) Morishita, R.; Gibbons, G. H.; Horiuchi, M.; Ellison, K. E.; Nakajima, M.; Zhang, L.; Kaneda, Y.; Ogihara, T.; Dzau, V. J. *Proc. Natl. Sci. U.S.A.* **1995**, *92*, 5855−5859.
(7) Morishita, R.; Sugimoto, T.; Aoki, M.; Kida, I.; Tomita, N.; Moriguchi, A.; Maeda, K.; Sawa, Y.; Kaneda, Y.; Higaki, J.; Ogihara, T. *Nature Med.* **1997**, *3*, 894−899.
(8) Khaled, A. R.; Butfiloski, E. J.; Sobel, E. S.; Schiffenbauer, J. *Cell. Immunol.* **1998**, *185*, 49−58.
(9) Ono, S.; Date, I.; Onoda, K.; Shiota, T.; Ohmoto, T.; Ninomiya, Y.; Asari, S.; Morishita, R. *Hum. Gene Ther.* **1998**, *9*, 1003−1011.
(10) Sharma, H. W.; Perez, J. R.; Higgins-Sochaski, K.; Hsiao, R.; Narayanan, R. *Anticancer Res.* **1996**, *16*, 61−69.
(11) Tomita, N.; Morishita, R.; Tomita, S.; Yamamoto, K.; Aoki, M.; Matsushita, H.; Hayashi, S.; Higaki, J.; Ogihara, T. *J. Hypertens.* **1998**, *16*, 993−1000.
(12) Tomita, N.; Morishita, R.; Lan, H. Y.; Yamamoto, K.; Hashizume, M.; Notake, M.; Toyosawa, K.; Fujitani, B.; Mu, W.; Nikolic-Paterson, D. J.; Atkins, R. C.; Kaneda, Y.; Higaki, J.; Ogihara, T. *J. Am. Soc. Nephrol.* **2000**, *11*, 1244−1252.
(13) Suzuki, J.; Morishita, R.; Amano, J.; Kaneda, Y.; Isobe, M. *Gene Ther.* **2000**, *7*, 1847−1852.
(14) Tomita, N.; Morishita, R.; Tomita, S.; Gibbons, G. H.; Zhang, L.; Horiuchi, M.; Kaneda, Y.; Higaki, J.; Ogihara, T.; Dzau, V. J. *Gene Ther.* **2000**, *7*, 1326−1332.
(15) Vos, I. H.; Govers, R.; Grone, H. J.; Kleij, L.; Schurink, M.; De Weger, R. A.; Goldschmeding, R.; Rabelink, T. J. *FASEB J.* **2000**, *14*, 815−822.
(16) Uhlmann, E.; Peyman, A. *Chem. Rev.* **1990**, *90*, 543−583.
(17) Chu, B. C. F.; Orgel, L. E. *Nucleic Acids Res.* **1992**, *20*, 5857−5858.
(18) Egholm, M.; Buchard, O.; Christensen, L.; Behrens, C.; Freier, S. M.; Driver, D. A.; Berg, R. H.; Kim, S. K.; Norden, B.; Nielsen, P. E. *Nature* **1993**, *365*, 566−568.
(19) Demidov, V. V.; Potaman, V. N.; Frank-Kamenetskii, M. D.; Egholm, M.; Buchard, O.; Sönnichsen, S. H.; Nielsen, P. E. *Biochem. Pharmacol.* **1994**, *48*, 1310−1313.
(20) Romanelli, A.; Pedone, C.; Saviano, M.; Bianch, N.; Borgatti, M.; Mischiati, C.; Gambari, R. *Eur. J. Biochem.* **2001**, *268*, 6066−6075.
(21) Petersen, M.; Nielsen, C. B.; Nielsen, K. E.; Jensen, G. A.; Bondensgaard, K.; Singh, S. K.; Rajwanshi, V. K.; Koskin, A. A.; Dahl, B. M.; Wengel, J.; Jacobsen, J. P. *J. Mol. Recognit.* **2000**, *13*, 44−53.
(22) Petersen, M.; Wengel, J. *Trends Biotechnol.* **2003**, *21*, 74−81.
(23) Crinelli, R.; Bianchi, M.; Gentilini, L.; Magnani, M. *Nucleic Acids Res.* **2002**, *30*, 2435−2443.
(24) Hikishima, S.; Minakawa, N.; Kuramoto, K.; Ogata, S.; Matsuda, A. *ChemBioChem* **2006**, *7*, 1970−1975.
(25) Bielenska, A.; Shivedasani, R. A.; Zhang, L.; Nabel, G. J. *Science* **1990**, *250*, 997−1000.
(26) Brown, D. A.; Kang, S.-H.; Gryaznov, S. M.; DeDionisio, L.: Heidenreich, O.; Sullivan, S.; Xu, X.; Nerenberg, M. I. *J. Biol. Chem.* **1994**, *269*, 26801−26805.
(27) Hosoya, T.; Takeuchi, H.; Kanesaki, Y.; Yamakawa, H.; Miyano-Kurosaki, N.; Takai, K.; Yamamoto, N.; Takaku, H. *FEBS Lett.* **1999**, *461*, 136−140.
(28) Erie, D.; Sinha, N.; Olson, W.; Jones, R.; Breslauer, K. *Biochemistry* **1987**, *26*, 7150−7159.
(29) Chu, B. C. F.; Orgel, L. E. *Nucleic Acids Res.* **1992**, *20*, 5857−5858.
(30) Lee, I. K.; Ahn, J. D.; Kim, H. S.; Park, J. Y.; Lee, K. U. *Curr. Drug Targ.* **2003**, *4*, 619−623.
(31) Erie, D. A.; Jones, R. A.; Olson, W. K.; Sinha, N. K.; Breslauer, K. J. *Biochemistry* **1989**, *28*, 268 −273.
(32) Ashley, G. W.; Kushlan, D. M. *Biochemistry* **1991**, *30*, 2927 −2933.
(33) For examples, see: (a) Cowart, M.; Benkovic, S. J. *Biochemistry* **1991**, *30*, 788−796. (b) Milton, J.; Connolly, B. A.; Nikiforov, T. T.; Cosstick, R. *J. Chem. Soc., Chem. Commun.* **1993**, 779−780. (c) Ferentz, A. E.; Keating, T. A.; Verdine, G. L. *J. Am. Chem. Soc.* **1993**, *115*, 9006−9014 and references cited therein. (d) Erlanson, D. A.; Chen, L.; Verdine, G. L. *J. Am. Chem. Soc.* **1993**, *115*, 12583−12584. (e) Kool, E. T. *Annu. Rev. Biophys. Biomol. Struct.* **1996**, *25*, 1−28. (f) Kool, E. T. *Acc. Chem. Res.* **1998**, *31*, 502−510.
(34) Murakami, A.; Yamamoto, Y.; Namba, M.; Iwase, R.; Yamaoka, T. *Bioorg. Chem.* **2001**, *29*, 223−233.
(35) Glick, G. D. *J. Org. Chem.* **1991**, *56*, 6746−6747.
(36) Osborne, S. E.; Völker, J.; Stevens, S. Y.; Breslauer, K. J.; Glick, G. D. *J. Am. Chem. Soc.* **1996**, *118*, 11993−12003.
(37) Tanaka, H.; Vickart, P.; Bertrand, J.-R.; Rayner, B.; Morvan, F.; Imbach, J.-L.; Paulin, D.; Malvy, C. *Nucleic Acids Res.* **1994**, *22*, 3069−3074.
(38) Stein, C. A.; Subasinghe, C.; Shinozuka, K.; Cohen, J. S. *Nucleic Acids Res.* **1988**, *16*, 3209−3221.
(39) Mischiati, C.; Borgatti, M.; Bianch, N.; Rutigliano, C.; Tomassetti, M.; Feriotto, G.; Gambari, R. *J. Biol. Chem.* **1999**, *274*, 33114−33122.
(40) Romanelli, A.; Pedone, C.; Saviano, M.; Bianchi, N.; Borgatti, M.; Mischiati, C.; Gambari, R. *Eur. J. Biochem.* **2001**, *268*, 6066−6075.
(41) Crinelli, R.; Bianchi, M.; Gentilini, L.; Magnani, M. *Nucleic Acids Res.* **2002**, *30*, 2435−2443.

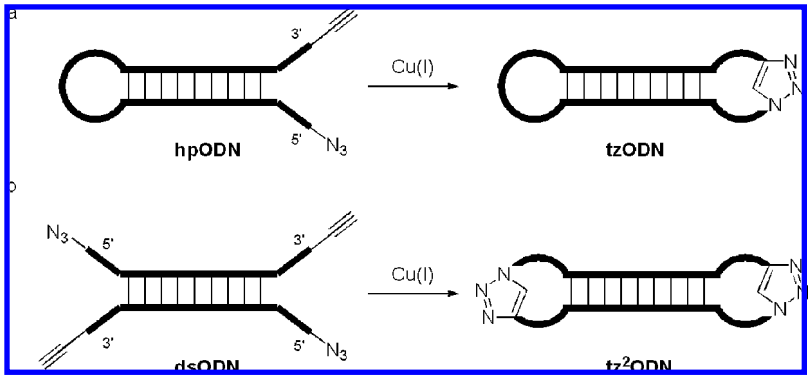

FIGURE 1. Formation of triazole cross-linked dumbbell-like ODNs (tzODN and tz^{2}ODN) by the cupper catalyzed alkyne−azide cycloaddition: (a) cross-linking of hairpin ODN (hpODN) at a single site and (b) cross-linking of double-stranded ODNs (dsODN) at both termini.

at room temperature, and affords a 1,4-disubstituted triazole selectively via a different reaction mechanism. Therefore, the CuAAC is a powerful linking reaction, due to its high degree of dependability, complete specificity, mild reaction conditions, and the bio-compatibility of the reactants, and has been increasingly used for in vivo and in vitro bioconjugation applications.[43−57] The CuAAC is also utilized in ODN bioconjugation and is suitable for terminal cross-linking of double-stranded ODNs.[43−54] Here we report the cross-linking of ODNs using the CuAAC as "a stable staple" to develop a novel strategy to synthesize decoy ODNs (Figure 1). To bridge the termini, we have alkylated the *N*-3 position of 2′-deoxythymidine with an azidoethyl and a propargyl group that permit the formation of an intramolecular triazole bridge.

Results and Discussion

First, a single-stranded hairpin hpODN **1** (Figure 2) was designed, where the azidoethyl and propargyl groups were attached at the *N*-3 positions of a thymine base at the 5′- and 3′-ends, to investigate the CuAAC at the single terminus as a model study (Figure 1a). Its synthesis is described in Scheme 1. The *N*-3-(iodoethyl)thymidine 3′-phosphoramidite **6** was devised as a precursor of the *N*-3-(azidoethyl)thymidine residue because azido groups are known to be readily reduced by a trivalent phosphorus atom, and thus the corresponding 3′-phosphoramidite block is impossible to prepare.[58] Once introduced in solid-phase DNA synthesis via the general phosphoramidite method, the iodo group was converted to the corresponding azide group via the on-column application of NaN_3. Treatment of 5′-*O*-(4,4′-dimethoxytrityl)thymidine (**1**) with allyl bromide and K_2CO_3 in DMF selectively gave the *N*-3-allyl derivative,

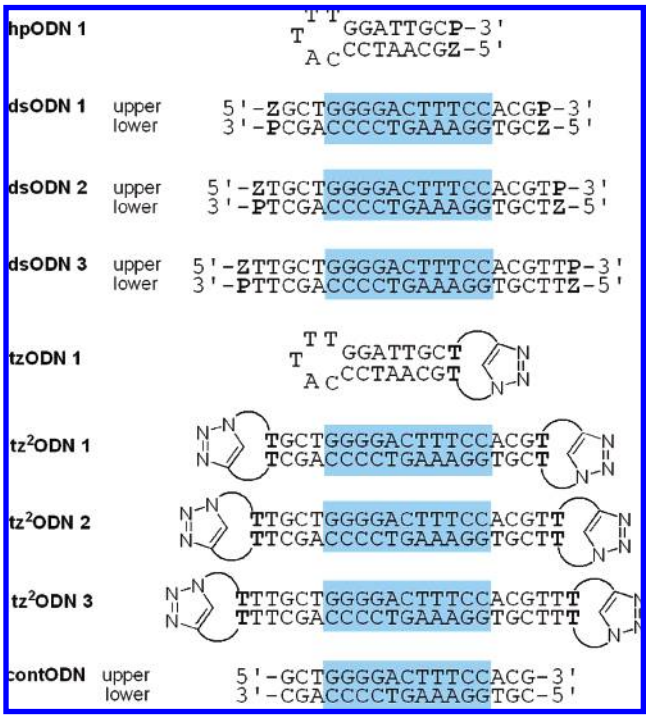

FIGURE 2. Sequences of the ODNs used in this study. **P** = *N*-3-(propargyl)thymidine residue; **Z** = *N*-3-(azidoethyl)thymidine residue; **T** = *N*-3-substituted thymidine residue. NF-κB recognition regions are marked with a gray box.

(42) (a) Tornøe, C. W.; Christensen, C.; Meldal, M. *J. Org. Chem.* **2002**, *67*, 3057−3064. (b) Rostovtsev, V. V.; Green, L. G.; Fokin, V. V.; Sharpless, K. B. *Angew. Chem., Int. Ed.* **2002**, *41*, 2596−2599. (c) Kolb, H. C.; Sharpless, K. B. *Drug Disc. Today* **2003**, *8*, 1128−1137.

(43) For review, see: (a) Kolb, H. C.; Finn, M. G.; Sharpless, K. B. *Angew. Chem., Int. Ed.* **2001**, *40*, 2004−2021. (b) Kolb, H. C.; Sharpless, K. B. *Drug Disc. Today* **2003**, *8*, 1128−1137.

(44) Seo, T. S.; Bai, X. P.; Ruparel, H.; Li, Z. M.; Turro, N. J.; Ju, J. Y. *Proc. Natl. Acad. Sci. U.S.A.* **2004**, *101*, 5488−5493.

(45) Punna, S.; Kuzelka, J.; Wang, Q.; Finn, M. G. *Angew. Chem., Int. Ed.* **2005**, *44*, 2215−2220.

(46) Kanan, M. W.; Rozenman, M. M.; Sakurai, K.; Snyder, T. M.; Liu, D. R. *Nature* **2004**, *431*, 545−549.

(47) Ustinov, A. V.; Korshun, V. A. *Russ. Chem. Bull.* **2006**, *55*, 1268−1274.

(48) Kumar, R.; El-Sagheer, A.; Tumpane, J.; Lincoln, P.; Wilhelmsson, L. M.; Brown, T. *J. Am. Chem. Soc.* **2007**, *129*, 6859−6864.

(49) Gierlich, J.; Burley, G. A.; Gramlich, P. M. E.; Hammond, D. M.; Carell, T. *Org. Lett.* **2006**, *8*, 3639−3642.

(50) Weller, R. L.; Rajski, S. R. *Org. Lett.* **2005**, *7*, 2141−2144.

(51) Seo, T. S.; Li, Z.; Ruparel, H.; Ju, J. *J. Org. Chem.* **2003**, *68*, 609−612.

(52) Byun, Y.; Al-Madhoun, A. S.; Johnsamuel, J.; Yang, W.; Barth, R. F.; Eriksson, S.; Tjarks, W. *J. Med. Chem.* **2005**, *48*, 1188−1198.

(53) Chan, T. R.; Hilgraf, R.; Sharpless, K. B.; Fokin, V. V. *Org. Lett.* **2004**, *6*, 2853−2855.

(54) Bouillon, C.; Meyer, A.; Vidal, S.; Jochum, A.; Chevolot, Y.; Cloarec, J.-P.; Praly, J.-P.; Vasseur, J.-J.; Morvan, F. *J. Org. Chem.* **2006**, *71*, 4700−4702.

(55) Burley, G. A.; Gierlich, J.; Mofid, M. R.; Nir, H.; Tal, S.; Eichen, Y.; Carell, T. *J. Am. Chem. Soc.* **2006**, *128*, 1398−1399.

(56) Chevolot, Y.; Bouillon, C.; Vidal, S.; Morvan, F.; Meyer, A.; Cloarec, J.-P.; Jochum, A.; Praly, J.-P.; Vasseur, J.-J.; Souteyrand, E. *Angew. Chem., Int. Ed.* **2007**, *46*, 2398−2402.

(57) Gogoi, K.; Mane, M. V.; Kunte, S. S.; Kumar, V. A. *Nucleic Acids Res.* **2007**, *35*, e139.

(58) Wada, T.; Mochizuki, A.; Higashiya, S.; Tsuruoka, H.; Kawahara, S.; Ishikawa, M.; Sekine, M. *Tetrahedron Lett.* **2001**, *42*, 9215−9219.

SCHEME 1. Preparation of hpODN 1 Containing *N*-3-(Propargyl)thymidine and *N*-3-(Azidoethyl)thymidine Derivatives[a]

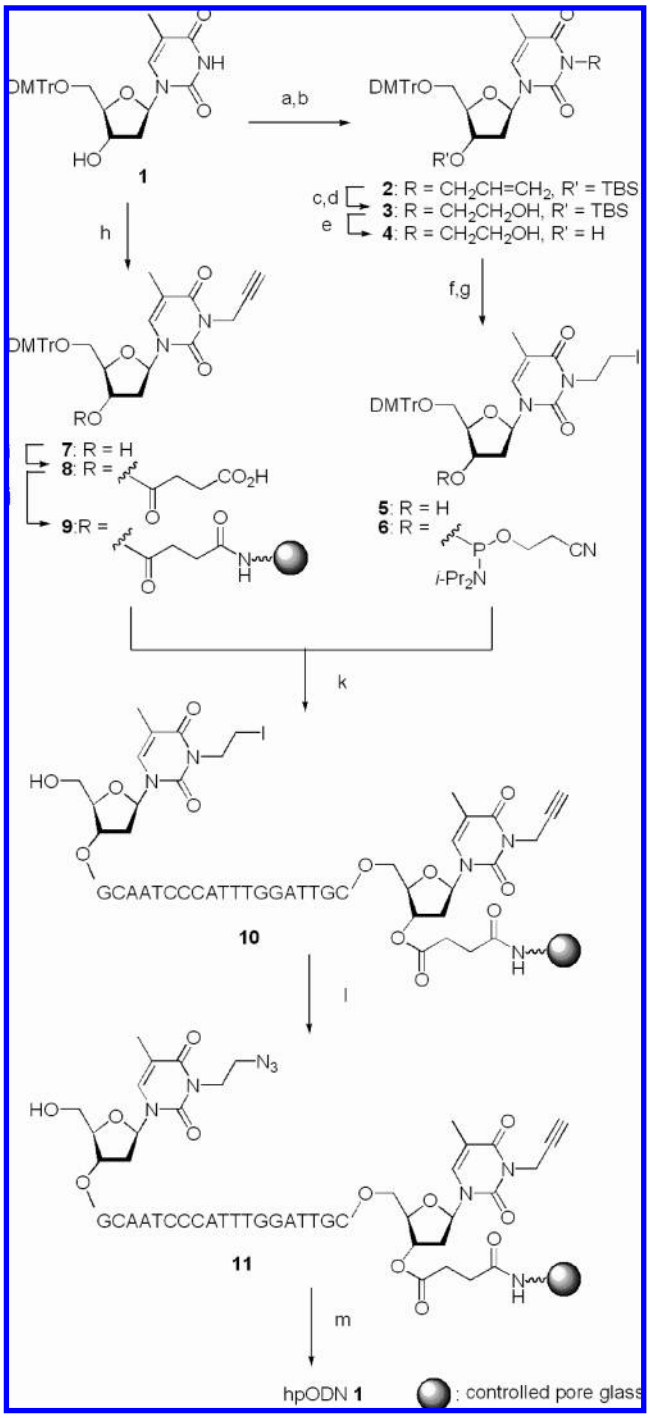

[a] Reagents and conditions: (a) allyl bromide, K_2CO_3, DMF, 91%; (b) TBSCl, imidazole, DMF, 90% in 2 steps; (c) OsO_4, NMO, aq acetone, then $NaIO_4$; (d) $NaBH_4$, MeOH, 71% in 2 steps; (e) TBAF, THF, 87%; (f) I_2, PPh_3, pyridine, toluene, 85%; (g) $NCCH_2CH_2OPClN$*i*-Pr_2, *i*-Pr_2NEt, CH_2Cl_2, 82%; (h) propargyl bromide, K_2CO_3, DMF, 93%; (i) succinic anhydride, DMAP, Et_3N, MeCN, quant.; (j) EDCl, amino-CPG, DMF, 34.2 μmol/g; (k) oligonucleotide synthesis; (l) NaN_3, DMF; (m) NH_4OH.

which was protected with a TBS protecting group (TBSCl, imidazole, DMF) at the 3′-position to afford **2**[59] in 90% yield in two steps. The allyl group of **2** was transformed into the desired hydroxyethyl group by a three-step sequence including dihydroxylation of the terminal olefin with OsO_4 and 4-methylmorpholine *N*-oxide in aqueous acetone, oxidative cleavage of the resulting diol with $NaIO_4$, and reduction of the resulting aldehyde derivative with $NaBH_4$ in MeOH to provide the *N*-3-hydroxyethyl derivative **3** in 71% yield in three steps. After the TBS group was removed (TBAF, THF, 87%), selective iodination of the primary hydroxyl group was conducted to give the corresponding *N*-3-iodoethyl derivative **5** (I_2, PPh_3, pyridine, toluene, 85%), which was converted to the conventional phosphoramidite block **6** ($NCCH_2CH_2OPClN$*i*-Pr_2, *i*-Pr_2NEt, CH_2Cl_2, 82%). The *N*-3-propargylthymidine linking to the controlled pore glass (CPG) **9** was also easily prepared by selective *N*-propargylation (propargyl bromide, K_2CO_3, DMF, 93%) followed by succinylation of the 3′-hydroxyl group of **7** (succinic anhydride, DMAP, Et_3N, MeCN, quant.) and attachment to the CPG (amino-CPG, EDCI, DMF, 34.2 μmol/g). Authentic triazole derivatives were also prepared as shown in Scheme 2. Thus, mesylation of the primary alcohol of **3** at the *N*-3 position and substitution with azide ion gave the corresponding *N*-3-(azidoethyl)thymidine derivative, which was sequentially deprotected to give *N*-3-(azidoethyl)thymidine (**Z**). *N*-3-(Propargyl)thymidine (**P**) was obtained by deprotection of the DMTr group in **7**. When an equimolar amount of **Z** and **P** was treated with $CuSO_4$ and sodium ascorbate in H_2O, 1,4-bisthymidine substituted 1,2,3-triazole **T-tz(1,4)-T** was produced selectively in 78% yield. On the other hand, the reaction of **Z** and **P** in the absence of Cu(I) catalyst in boiling water gave a mixture of **T-tz(1,4)-T** and its regioisomer **T-tz(1,5)-T** (62% for **T-tz(1,4)-T,** 23% for **T-tz(1,5)-T**, **T-tz(1,4)-T**/**T-tz(1,5)-T** = 2.7/1). The CPG-supported oligonucleotide **10** containing *N*-3-(iodoethyl)thymidine at the 5′-terminus and *N*-3-(propargyl)thymidine (**P**) at the 3′-terminus was synthesized on a DNA synthesizer in the DMTr-off mode. The CPG linking to ODN **10** was treated with NaN_3 in DMF (0.5 M) for 12 h at room temperature to give **11**. After azidation, the ODN was released from the CPG and deprotected, and the resulting crude product was purified by reverse-phase HPLC to give hpODN **1** (Figure 3a), which was characterized by analysis of the nucleoside composition by enzymatic digestion using snake venom phosphodiesterase (SVPD) and calf intestine alkaline phosphodiesterase (Figure 4b). Two peaks corresponding to the authentic **P** and **Z** were observed in the HPLC chart of the reaction mixture, and the ratio of the peak intensity of **P** to that of **Z** was 1.0, which was the theoretical value.

For the cross-linking reactions of hpODN **1**, the Cu(I) catalyst was prepared in situ from Cu(II) sulfate and sodium ascorbate. After the annealing of the hpODN **1**, the CuAAC was carried out by adding 10 equiv of $CuSO_4$ to a solution of hpODN **1** (0.1 M) in 0.1 M MOPS buffer (pH 7.0) containing 5 mM sodium ascorbate and 1 M NaCl at room temperature for 12 h and resulted in complete consumption of the hpODN **1**. However, extensive degradation of the ODN occurred under these conditions, a problem that has been encountered previously.[46] Since as was reported in the literature, the tris(benzyltriazolyl)amine (TBTA) ligand[53] greatly reduces degradation of ODNs,[48] we therefore decided to investigate the use of the TBTA ligand in our system. A premixed $CuSO_4$−TBTA complex (10 equiv) was added to a solution of hpODN **1** and sodium ascorbate in the same buffer, giving the triazole cross-linked tzODN **1** by HPLC analysis (93%, Figure 3b). The

(59) Hayakawa, Y.; Hirose, M.; Noyori, R. *J. Org. Chem.* **1993**, *58*, 5551−5555.

SCHEME 2. Preparation of 1,4- and 1,5-Bisthymidine-Substituted Triazole Derivatives

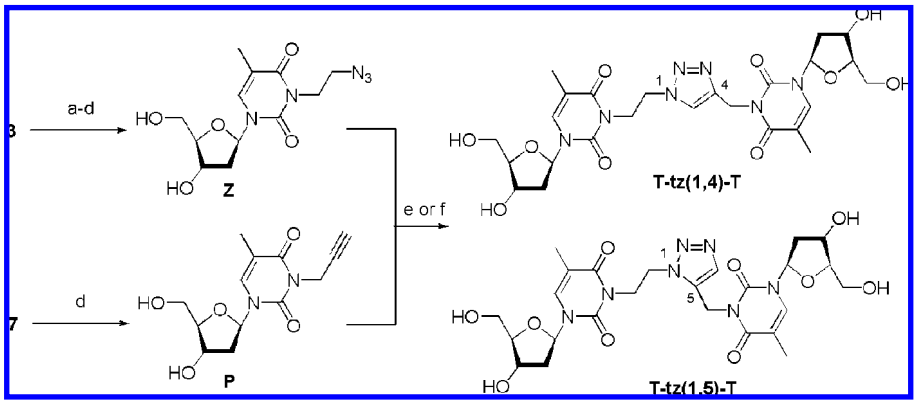

[a] Reagents and conditions: (a) MsCl, pyridine; (b) NaN_3, DMF; (c) TBAF, THF, 85% in 3 steps; (d) 80% aq AcOH, 85% for **Z**, 97% for **P**; (e) $CuSO_4$, sodium ascorbate, H_2O, 78% (**T-tz(1,4)-T**); (f) H_2O, reflux, 62% (**T-tz(1,4)-T**), 23% (**T-tz(1,5-T**).

progress of the reaction was also monitored by denaturing polyacrylamide gel electrophoresis (Figure 5a). After addition of the $CuSO_4$−TBTA complex to a solution of the ODN and sodium ascorbate, a new band was observed with higher mobility than that of the starting hpODN **1,** and the reaction was complete in about 4 h according to electrophoretic analysis. This clearly showed the formation of a cyclic product with higher gel-mobility than the linear starting hpODN **1**, as generally observed for circular ODNs by denaturing gel electrophoresis. The resulting tzODN **1** was purified by reverse-phase HPLC, and enzymatic digestion of the ODN showed that the 1,4-disubstituted triazole-bridged thymidine dimer **T-tz-(1,4)-T** was contained in the ODN, which was identical with the authentic material by HPLC analysis (Figure 4a,c). The resulting nucleoside composition was in good accordance with the desired one. In the absence of Cu(I) catalyst, the reaction generally proceeds under thermal conditions or when both the azide and acetylene groups would be in close proximity. In these instances, a regioisomeric mixture of 1,4-disubstituted and 1,5-disubstituted triazoles should be obtained. In our study, only the 1,4-disubstituted triazole-bridged thymidine dimer **T-tz-(1,4)-T** was detected in the enzymatic digestion experiment, and the corresponding 1,5-disubstituted triazole derivative **T-tz-(1,5)-T** was not seen at all. The triazole cross-linked ODN was not observed during the annealing process, and no reaction was noted without the presence of the Cu(I) catalyst when the precursor ODN (such as hpODN **1**) in the reaction buffer was left for several weeks at room temperature. These results clearly show that the cross-linking reaction between the 3′- and 5′-positions of the ODN by the CuAAC successfully proceeded on the addition of the Cu(I) catalyst.

Having established conditions for the terminal cross-linking of hairpin ODNs by the CuAAC, we applied this method to the assemblage of a double-stranded ODN with the covalent triazole cross-linking providing dumbbell ODNs, which would act as *cis*-elements against NF-κB. Several *cis*-element sequences of NF-κB consisting of 10 base pairs are known to exist. To install stem sequences at both termini of the double-stranded ODNs, it would be necessary to prepare relatively long single-stranded ODNs, the preparation and isolation of which are quite often troublesome when the required sequences are relatively long. Another strategy for designing dumbbell ODNs would be by terminal cross-linking, namely, the preparation of relatively short complementary single-stranded ODNs, which are annealed to form double-stranded ODNs, with terminal cross-linking at both termini conducted simultaneously (Figure 1b). Owing to the facile preparation of each single-stranded ODNs, this method allows us to prepare a relatively long dumbbell ODNs. With this in mind, we decided to investigate the triazole cross-linking of double-stranded ODNs at both termini, although it proved to be challenging. Constraining the double-stranded ODNs by terminal cross-linking could cause structural deformation and/or limit conformational flexibility. Protein−nucleic acid interactions sometimes involve an induced-fit in their binding, and their affinity would be reduced with double-stranded DNAs with a constrained conformation. However, increasing the size of the loop might reduce the constraint within double-stranded ODNs. Therefore, we designed a series of dsODNs **1**−**3** (Figure 2) that contained an 11-mer NF-κB binding sequence with **Z** and **P** at the 3′- and 5′-termini, respectively, while varying the number of the terminal thymidine residues to observe the impact of the loop size on the cross-linking reaction and the NF-κB binding ability. The nucleotide sequence corresponding to a single asymmetric NF-κB binding site of the HIV-1 RTL was chosen to minimize potential problems related to self- and/or intrastrand hybridization as previously investigated.[27] In a manner similar to the preparation of the model hpODN **1**, dsODNs **1**−**3** were synthesized and purified, and their structure was confirmed by analysis of nucleoside composition by enzymatic digestion (data not shown). With these dsODNs in hand, we then conducted the triazole cross-linking at both termini. DsODNs **1**−**3** were prepared by annealing equimolar amounts of the corresponding single-stranded ODNs in a 0.1 M MOPS buffer (pH 7.0) containing 1 M NaCl (each ODN concentration was 0.1 M). The CuAAC of dsODN **1** was carried out under the same conditions as for the one with hpODN **1** and monitored by denaturing polyacrylamide gel electrophoresis (Figure 5b). After the $CuSO_4$−TBTA complex was added, a new band with lower mobility than that of the starting dsODN **1** was observed, and the reaction was complete within 4 h. The reaction proceeded efficiently (Figure 3c,d), and the desired triazole cross-linked ODN, tz^2ODN **1**, was obtained after HPLC purification. The conversion was 95% by HPLC analysis. The structure of tz^2-ODN **1** was also confirmed by enzymatic digestion to be the same as tzODN **1**. Thus, no peaks corresponding to **Z** and **P** were detected by HPLC analysis, and the 1,4-disubstituted triazole-bridged thymidine dimer **T-tz(1,4)-T** was formed instead (Figure 4d). This would imply that the triazole cross-linking indeed occurred at both termini providing a dumbbell-

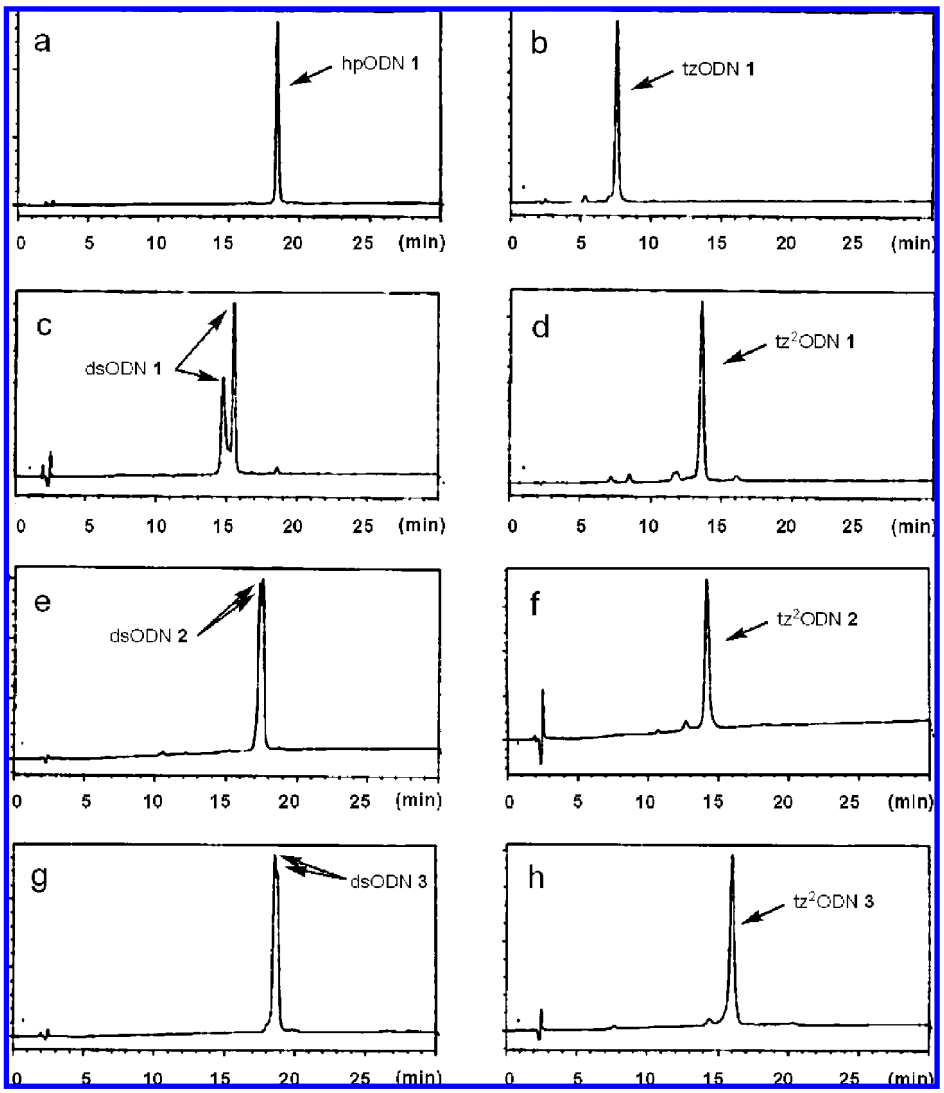

FIGURE 3. Denaturing reverse-phase HPLC chromatograms (UV absorbance vs time) of the cross-linking reaction of hpODN **1** and dsODNs **1**, **2**, and **3**: (a) hpODN **1** in the absence of Cu[I] catalysis; (b) after the CuAAC of hpODN **1**; (c) dsODN **1** in the absence of Cu[I] catalysis; (d) after the CuAAC of dsODN **1**; (e) dsODN **2** in the absence of Cu[I] catalysis; (f) after the CuAAC of dsODN **2**; (g) dsODN 3 in the absence of Cu[I] catalysis; (h) after the CuAAC of dsODN **3**. All the reactions were performed with 50 μM ODN in 100 mM NOPS−NaOH (pH 7, 1 M NaCl−^{t}BuOH) in the presence of 500 mM $CuSO_4$−TBTA complex and 5 mM sodium ascorbate for 6 h to afford tzODN **1** and tz^{2}ODN **1**, **2**, and **3** (indicated as arrows), respectively.

like ODN. In a manner similar to the cross-linking reaction of dsODN **1**, the CuAAC of the dsODNs **2** and **3**, which possess extra thymidine residues at both termini, proceeded smoothly to provide tz^{2}ODNs **2** (Figures 3e,f and 4e) and **3** (Figures 3g,h and 4f), respectively.

CD spectroscopy was used to study the macroscopic helical geometry of the chemically modified tz^{2}ODNs **1**−**3** together with the natural double-stranded control ODN (contODN). The natural double-stranded 17-mer ODN (contODN) displayed a characteristic B-DNA spectrum possessing a positive ellipticity at 283 nm, a negative ellipticity at 252 nm, and a crossover between 255 and 262 nm (Figure 6).[60] Tz^{2}ODNs **1**−**3** possessing the triazole cross-linked thymidines at both ends of the helix displayed an increase in positive amplitude at 283 nm and an increase in the negative one without any other significant changes in the overall CD spectrum. A similar CD characteristic was observed in double-stranded ODNs possessing disulfide bridges at the termini in a study by Glick et al.[36] They speculated that differences in the CD spectra between a natural ODN and the cross-linked ODN may simply arise from inherent differences in the composition of the sequences, or the increase in ellipticity at 283 nm may be related to an increased winding of the helix induced by the presence of the thymidine bases. It could also be speculated that, due to its analogous structure, our triazole cross-linked ODNs would also possess similar properties. Nevertheless, the general correspondence in the CD curves suggests that the terminal base modifications do not significantly distort the helical geometry of the duplex.

UV melting experiments were next conducted to characterize the thermally induced denaturation of tz^{2}ODNs with the goal of elucidating the thermal consequences of modifying and constraining DNA via the triazole cross-linking (Table 1). The T_m values for tz^{2}ODNs **1**−**3** were 89.8, 85.2, and 81.7 °C, respectively. An increase in the number of thymidine residues

(60) Ivanov, V. I.; Minchenkova, L. E.; Schyolkina, A. K.; Poletayev, A. I. *Biopolymers* **1973**, *12*, 89−110.

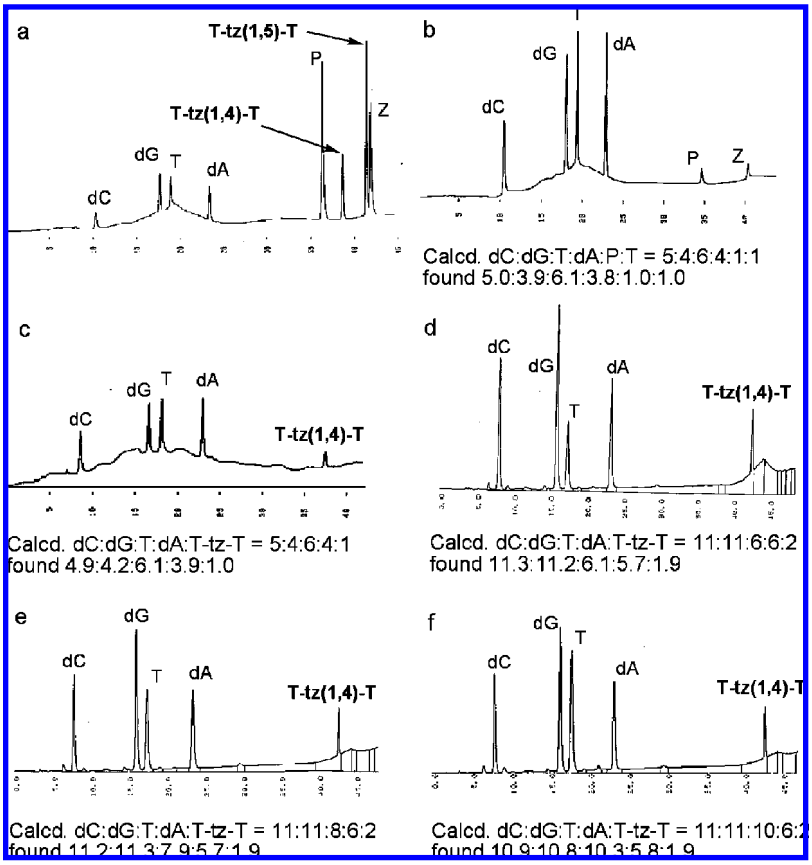

FIGURE 4. HPLC profiles (UV absorbance vs time) of enzymatic digestion of ODNs and their nucleoside compositions: (a) A mixture of authentic nucleosides; (b) hpODN **1**; (c) tz^{2}ODN **1**; (d) tz^{2}ODN **1**; (e) tz^{2}ODN **2**; and (f) tz^{2}ODN **3**.

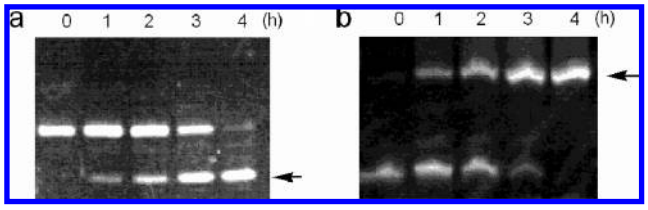

FIGURE 5. Denatured polyacrylamide gel electrophoresis of the cross-linking reaction of (a) hpODN **1** and (b) dsODN **1**. Arrows indicate triazole-cross-linked ODNs.

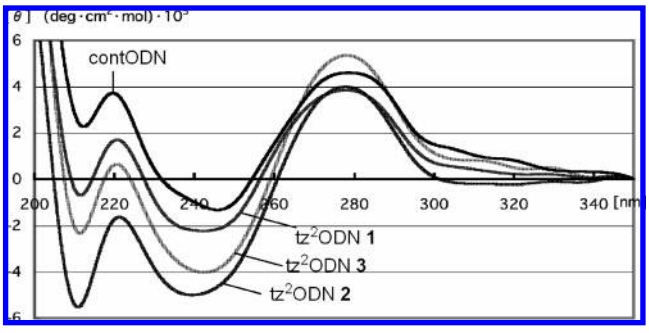

FIGURE 6. Circular dichroism spectra (conditions: 2 μM of ODN in sodium cacodylate−HCl buffer (1 mM, pH 7.0) containing 10 mM NaCl) of contODN and tz^{2}ODN **1**−**3**.

in the loops resulted in a decrease in thermal stability. Comparing the T_m values for cross-linked tz^{2}ODNs (81.7−89.8 °C) with those of the control double-stranded ODN (55.7 °C) revealed a dramatic increase in thermal stability with

TABLE 1. Thermal Stability of the Triazole Cross-Linked Dumbbell ODNs

	T_m (°C)[a]	ΔT_m (°C)[b]
contODN	55.7	
dsODN **1**	52.7	−3.0
dsODN **2**	50.3	−5.4
dsODN **3**	47.0	−8.7
tz^{2}ODN **1**	89.8	+34.1
tz^{2}ODN **2**	85.2	+29.5
tz^{2}ODN **3**	81.7	+26.0

[a] Conditions: 3 μM each ODN, 1 mM sodium cacodylate−HCl (pH 7.0), 1 mM NaC1. Average of three measurements. [b] T_m(modified) − T_m(control).

the triazole cross-link, and it is estimated that the double triazole cross-link results in an increase in thermal stability ranging from 26 to 34 °C, which is similar to that of a disulfide cross-linked 12-mer ODN (38.1 °C) reported by Glick et al., although the sequence and length of the ODN were different.[35,36]

Cleavage by a 3′-exonuclease, the activity of which is predominant in human serum,[6] was next examined since an enzyme recognition site is proximal to our modified thymidines. Snake venom phosphodiesterase (SVPD) degrades DNA from the 3′-end of a double-stranded DNA releasing 5′-dNMPs.[61] Cross-linking on the terminal bases leaves the terminal hydroxyls available for [^{32}P]-end-labeling by a standard procedure used in ODN chemistry. SVPD degrades the control ODN rapidly ($t_{1/2}$ of 10.4 ± 2.4 min, Figure 7a). On the other hand,

(61) Williams, E. J.; Sung, S.-C.; Laskowski, M., Sr. *J. Biol. Chem.* **1961**, *236*, 1130−1134.

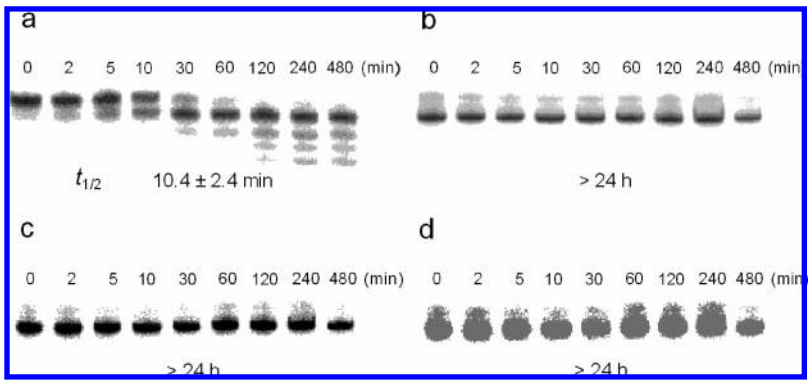

FIGURE 7. Susceptibility to snake venom phosphodiesterase degradation of triazole cross-linked dumbbell ODNs: (a) contODN; (b) tz^{2}ODN **1**; (c) tz^{2}ODN **2**; and (d) tz^{2}ODN **3**. 5′-^{32}P-labeled control contODN and tz^{2}ODNs **1**−**3** were incubated for different lengths of time, as indicated, with 64 μU snake venom phosphodiesterase in 40 mM Tris-HCl buffer (pH 7.5) at 37 °C and then submitted to electrophoretic separation on 20% denatured polyacrylamide gels.

tz^{2}ODNs **1**−**3** were revealed to be totally resistant to SVPD degradation, and the apparent half-lives are 500-fold greater ($t_{1/2}$ > 24 h, Figure 7b−d). These data suggest that the nucleolytic activity may require the enzyme to partially expose phosphodiester bonds near the 3′-side[62] by unwinding or "melting" the helix upon binding, which is limited by the topological constraint imposed by the cross-link.[36,63,64] In conjunction with increased thermal stability, the newly synthesized dumbbell ODNs possess suitable properties required for biological application of decoy molecules.

With the synthetic strategy and the basic structural and nuclease resistant properties of the ODNs established, the ability of tz^{2}ODNs **1**−**3** to bind with NF-κB was investigated by electrophoretic mobility shift assays (EMSA) in a procedure similar to that reported previouly.[65] ^{32}P-labeled ODNs were incubated with various amounts of NF-κB p50 homodimer at 0 °C for 30 min, and the mixture was analyzed by gel electrophoresis. A single protein−ODN complex migrating with the same electrophoretic mobility was observed with all probes as well as with the control ODN, as shown in Figure 8. The results indicated that formation of the protein−ODN complexes had occurred. Apparent dissociation constants (K_d) of tz^{2}ODNs **1**−**3** were determined to be 18 ± 4, 14 ± 1, and 9 ± 2 nM, respectively, and these ODNs exhibited a similar binding affinity to that of the control decoy ODN (12 ± 3 nM). Furthermore, formation of the complex of ^{32}P-labeled control ODN and the NF-κB p50 homodimer was competitively inhibited by addition of unlabeled tz^{2}ODNs **1**−**3** in a dose-dependent fashion, and their IC_{50} values were 3.9 ± 0.5 nM for tz^{2}ODN **1**, 2.6 ± 0.3 nM for tz^{2}ODN **2**, and 3.0 ± 0.5 nM for tz^{2}ODN **3** (Figure 9). This would indicate that the newly synthesized dumbbell ODNs were recognized by NF-κB p50 homodimer in a manner similar to that of the control decoy ODN and that they act as decoy molecules. Of particular interest is the observation of different binding of the synthesized modular dumbbell ODNs to the protein. Comparison of the dumbbell ODNs with their binding properties to NF-κB reveals some important differences. Tz^2-ODN **3** with six-base loops has the highest binding affinity

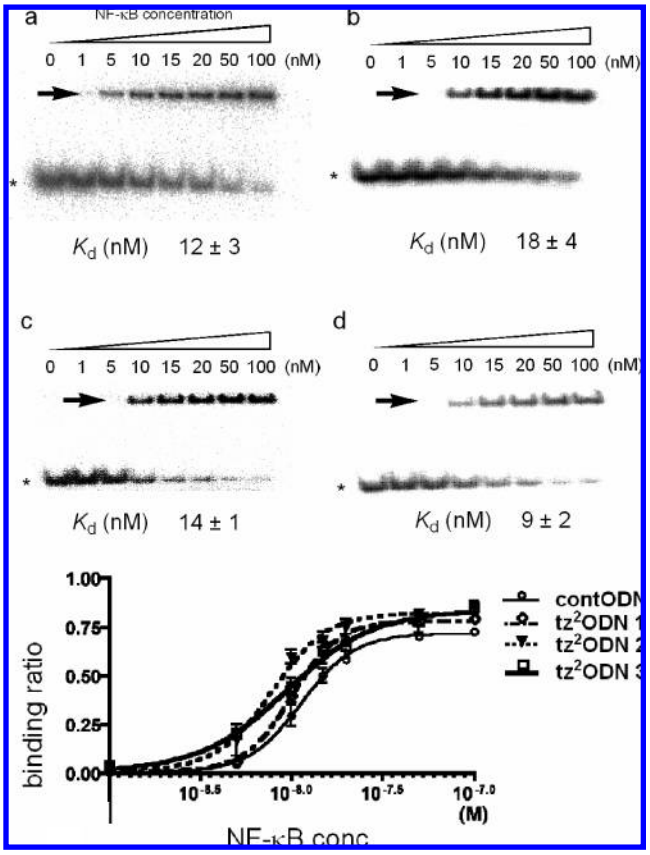

FIGURE 8. Effects of the triazole cross-linked dumbbell ODNs on the interaction with the NF-κB p50 homodimer and the electromobility shift assay with NF-κB. ^{32}P-radiolabeled triazole cross-linked dumbbell ODNs (40 fmol) was incubated at 0 °C for 30 min in 10 mM HEPES buffer (pH 7.5) in the presence of the indicated concentration of NF-κB p50 homodimer: (a) contODN; (b) tz^{2}ODN **1**; (c) tz^{2}ODN **2**; and (d) tz^{2}ODN **3**. Protein−ODN complexes are marked with an arrow. (e) Binding curves with NF-κB and triazole cross-linked dumbbell ODNs. Each dissociation constant was calculated by three independent experiments and shown as average ±S.E.

among the three dumbbell ODNs, and the greater the number of thymidine residues constituting the loop region, the higher the binding affinity of the dumbbell ODNs to the NF-κB, although the magnitude is subtle. Recently, several solution structures of free DNAs containing NF-κB recognition sequences and their complexes with NF-κB dimer have been

(62) Tarköy, M.; Leumann, C. *Angew. Chem., Int. Ed. Engl.* **1993**, *32*, 1432−1434.
(63) Cowart, M.; Gibson, K. J.; Allen, D. J.; Benkovic, S. J. *Biochemistry* **1989**, *28*, 1975−1983.
(64) Catalano, C. E.; Benkovic, S. J. *Biochemistry* **1989**, *28*, 4374−4382.
(65) Murata, S.; Mizumura, Y.; Hino, K.; Ueno, Y.; Ichikawa, S.; Matsuda, M. *J. Am. Chem. Soc.* **2007**, *129*, 10300−10301.

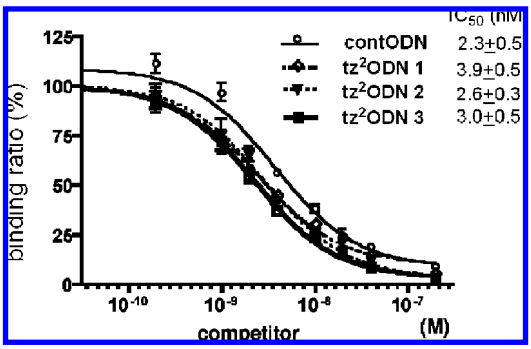

FIGURE 9. Competition curves of triazole cross-linked dumbbell ODNs for binding of NF-κB p50 homodimer to radiolabeled control ODN. Competition experiments were performed by incubating NF-κB p50 homodimer (40 fmol) together with the ^{32}P-radiolabeled ODN (40 fmol) and the competitor ODNs. IC_{50} values for each type of competitor were estimated by plotting these data as a competitor concentration (M) and fitting to a dose−response curve. Each IC_{50} value was calculated by three independent experiments and shown as average ±S.E.

reported.[66−70] These structures allow investigation of the role of DNA conformation on specific NF-κB dimer recognition and binding. It is suggested that the NF-κB family discriminates the subtle structural alteration of *trans*-elements including hydration, bending, and unwinding. It can be speculated that the terminal cross-link might result in some structural changes even in internal double-stranded structures of the ODNs without significantly changing CD spectra. ODNs with shorter loops have more reduced conformational flexibility. As a result, their binding affinity with the protein is reduced compared to the parent unmodified decoy ODN because they cannot adopt a structural alteration suitable for protein binding. Increasing the size of the loop might reduce the constraint within double-stranded ODNs to recover conformational flexibility.

Conclusion

Triazole-cross-linked ODNs were synthesized using the CuAAC with hairpin DNA possessing *N*-3-(azidoethyl)thymidine and *N*-3-(propargyl)thymidine at the 3′- and 5′-termini. The newly synthesized ODNs were thermally stable and their structures resembled those of non-cross-linked ODNs. This strategy is effective for the preparation of cross-linked ODNs because the precursor ODNs are stable and easy to prepare, and the cross-link reactions proceed chemoselectively. The newly synthesized dumbbell ODNs possess good properties, including excellent stability against exonuclease and high thermal stability, which are necessary for the decoy molecules in order to achieve biological responses leading to alteration of gene expression. It was also demonstrated that the dumbbell ODNs have the ability to bind to NF-κB p50 homodimer within a range similar to that of the control decoy ODN. Our methodology allows us to prepare dumbbell ODNs with various loop lengths. This study clearly shows that the cross-linking by the triazole structure does not prevent the dumbbell ODNs from binding to the NF-κB transcription factor. Therefore, the results obtained conclusively demonstrate that the triazole cross-linked dumbbell ODNs can be proposed as powerful decoy molecules.

Experimental Section

1-(2-Deoxy-β-D-ribofuranosyl)-3-(2-azidoethyl)thymine (Z). A solution of 1-[2-deoxy-5-*O*-(4,4′-dimethoxytrityl)-β-D-ribofuranosyl]-3-(2-azidoethyl)thymine (97 mg, 0.16 mmol) in 80% aqueous AcOH (10 mL) was stirred for 2 h at room temperature. The mixture was concentrated in vacuo, and the resulting residue was co-evapolated with EtOH (3×). The residue was purified by a silica gel column (50−100% AcOEt−hexane) to afford **Z** (45 mg, 91%) as a white powder. For analysis, a part of the material was crystallized from AcOEt−hexane (mp 82 °C): ^{1}H NMR (400 MHz, $CDCl_3$) δ 7.37 (s, 1H), 6.18 (dd, 1H, J = 6.4, 7.3 Hz), 4.59 (m, 1H), 4.19 (t, 2H, J = 6.2 Hz), 4.01 (m, 1H), 3.94 (dd, 1H, J = 2.8, 11.9 Hz), 3.84 (dd, 1H, J = 3.1, 11.9 Hz), 3.53 (t, 2H, J = 6.2 Hz), 2.50, 2.29 (each s, each br s), 2.43 (ddd, 1H, J = 3.8, 6.4, 13.7 Hz), 2.33 (ddd, 1H, J = 6.4, 7.3, 13.7 Hz), 1.94 (s, 3H); ^{13}C NMR (100 MHz, $CDCl_3$) δ 12.5, 40.0, 40.2, 48.4, 62.4, 71.4, 86.9, 87.0, 110.3, 135.1, 150.9, 163.2; UV (λ_{max} = 268 nm, ϵ_{260} = 7910 M^{-1} cm^{-1}, ϵ_{268} = 9050 M^{-1} cm^{-1}). Anal. Calcd for $C_{12}H_{17}N_5O_5$: C, 46.30; H, 5.50; N, 22.50. Found: C, 46.56; H, 5.46; N, 22.08. LRMS (FAB) *m*/*z* 312 (MH^+); HRMS (FAB) calcd for $C_{12}H_{18}N_5O_5$ (MH^+) 312.1308, found 312.1313.

1-(2-Deoxy-β-D-ribofuranosyl)-3-(2-propynyl)thymine (P). A solution of **7** (400 mg, 0.68 mmol) in 80% aqueous AcOH (10 mL) was stirred for 2 h at room temperature. The mixture was concentrated in vacuo, and the resulting residue was co-evapolated with EtOH (3×). The residue was purified by a silica gel column (0−4% MeOH−$CHCl_3$) to afford **P** (190 mg, 97%) as a white powder. For analysis, a part of the material was crystallized from AcOEt−hexane (mp 87−88 °C). The data were identical in all respects with the properties previously reported:[71] ^{1}H NMR (400 MHz, $CDCl_3$) δ 7.45 (s, 1H), 6.24 (t, 1H, J = 6.8 Hz), 4.70 (d, 2H, J = 1.8 Hz), 4.59 (m, 1H), 4.02 (m, 1H), 3.93 (dd, 1H, J = 2.8, 11.9 Hz), 3.85 (dd, 1H, J = 2.4, 11.9 Hz), 2.55 (m, 2H), 2.38 (m, 2H), 2.18 (d, 1H, J = 1.8 Hz), 1.95 (s, 3H); UV (λ_{max} = 268 nm, ϵ_{260} = 8090 M^{-1} cm^{-1}, ϵ_{268} = 9060 M^{-1} cm^{-1}). Anal. Calcd for $C_{13}H_{16}N_2O_5$: C, 55.71; H, 5.75; N, 9.99. Found: C, 55.56; H, 5.75; N, 10.00.

Cycloaddition in the Presence of Cu(I) Catalyst. Sodium ascorbate (5 mg, 50 μmol) and an aqueous solution of $CuSO_4$ (10 mM, 1 mL, 10 μmol) were added to a solution of **Z** (31 mg, 0.10 mmol) and **P** (28 mg, 0.10 mmol) in H_2O (1 mL), and the mixture was stirred for 8 h at room temperature. The mixture was concentrated in vacuo, and the residue was purified by a silica gel column (10% MeOH−$CHCl_3$) to afford **T-tz(1,4)-T** (46 mg, 78%) as a white powder: ^{1}H NMR (500 Hz, CD_3OD) δ 7.88 (s, 1H), 7.85, 7.80 (each s, each 1H), 6.31, 6.12 (each m, each 1H), 5.17 (s, 2H), 4.64 (s, 2H), 4.35 (m, 4H), 3.91 (m, 2H), 3.82−3.70 (m, 4H), 2.28−2.14 (m, 4H), 1.92, 1.83 (each s, each 3H); ^{13}C NMR (100 MHz, $CDCl_3$) δ 13.9, 14.0, 37.7, 42.2, 42.3, 42.5, 63.4, 63.5, 72.6, 72.8, 88.0, 88.1, 89.6, 111.2, 111.5, 126.7, 137.5, 145.5, 152.7, 152.8, 165.7, 165.8; UV (λ_{max} = 268 nm, ϵ_{260} = 13400 M^{-1} cm^{-1}, ϵ_{268} = 15200 M^{-1} cm^{-1}); LRMS (FAB) *m*/*z* 592 (MH^+); HRMS (FAB) calcd for $C_{25}H_{34}N_7O_{10}$ (MH^+) 592.2367, found 592.2379.

Cycloaddition under Thermal Conditions. A solution of **Z** (31 mg, 0.10 mmol) and **P** (28 mg, 0.10 mmol) in H_2O (1 mL) was heated under reflux for 8 days. The mixture was concentrated in vacuo, and the residue was purified by a silica gel column (1−14% MeOH−$CHCl_3$) to afford **T-tz(1,4)-T** (37 mg, 62%) as a white powder and **T-tz(1,5)-T** (13 mg, 23%) as a white powder. Data

(66) Muller, C. W.; Harrison, S. C. *FEBS Lett.* **1995**, *369*, 113−117.
(67) Ghosh, G.; van Duyne, G.; Ghosh, S.; Sigler, P. B. *Nature* **1995**, *373*, 303−310.
(68) Chen, F. E.; Huang, D. B.; Chen, Y. Q.; Ghosh, G. *Nature* **1998**, *391*, 410−413.
(69) Chen, Y. Q.; Ghosh, S.; Ghosh, G.; Cramer, P.; Larson, C. J.; Verdine, G. L.; Muller, C. W. *EMBO J.* **1997**, *16*, 7078−7090.
(70) Huang, D.-B.; Phelps, C. B.; Fusco, A. J.; Ghosh, G. *J. Mol. Biol.* **2005**, *346*, 147−160.
(71) Byun, Y.; Al-Madhoun, A. S.; Johnsamuel, J.; Yang, W.; Barth, R. F.; Eriksson, S.; Tjarks, W. *J. Med. Chem.* **2005**, *48*, 1188−1198.

for **T-tz(1,5)-T**: ^{1}H NMR (500 Hz, CD_3OD) δ 7.88, 7.81 (each s, each 1H), 7.64 (s, 1H), 6.31, 6.11 (each m, each 1H), 5.33, 5.29 (each d, each 1H, J = 15.1 Hz), 4.91 (s, 2H), 4.39 (m, 4H), 3.92 (m, 2H), 3.80−3.73 (m, 4H), 2.28−2.13 (m, 4H), 1.94, 1.85 (each s, each 3H); ^{13}C NMR (100 MHz, $CDCl_3$) δ 13.8, 13.9, 34.4, 42.1, 42.2, 42.3, 47.5, 63.5, 72.6, 72.7, 88.1, 89.6, 89.7, 111.1, 111.4, 136.2, 136.7, 137.5, 137.8, 152.8, 165.7; LRMS (FAB) *m*/*z* 592 (MH^+); HRMS (FAB) calcd for $C_{25}H_{34}N_7O_{10}$ (MH^+) 592.2367, found 592.2358.

Preparation of Cross-Linking Precursor Oligodeoxynucleotides. Oligonucleotides containing *N*-3-(iodoethyl)thymidine at the 5′-terminus and *N*-3-(propargylethyl)thymidine (**P**) at the 3′-terminus were synthesized on a DNA synthesizer (Applied Biosystems Model 3400) in the DMTr-off mode, as we previously reported.[24] CPG supporting ODNs was treated with 0.5 M NaN_3 in DMF (2 mL) at room temperature for 12 h. The CPG was filtrated, washed successively with ethanol and acetone, and dried. ODNs were released from CPG by treatment with 28% aqueous ammonia at 55 °C for 16 h, and the resulting solution was concentrated and purified by reverse-phase HPLC using a linear gradient of 5−20.75% MeCN in 0.1 M TEAA buffer (pH 7.0).

CuAAC of ODNs. A solution of a duplex (25 nmol) composed of two oligodeoxynucleotides was heated in 100 mM MOPS−NaOH buffer (pH 7.0) containing 1 M NaCl at 90 °C for 1 min and allowed to cool to room temperature for 4 h. A solution of $CuSO_4$−tris(benzyltriazolyl)amine[53] (TBTA) in 50% aqueous *t*-BuOH (28 mM, 9 μL, 250 nmol) and sodium ascorbate (2.5 μmol) was sequentially added to a solution of the duplex, and the mixture was incubated at 25 °C for 12 h. Hydrogen sulfide gas was passed through the reaction mixture, which was washed with chloroform (3×). The aqueous solution was desalted on a NAP-25 column (GE Healthcare) and then lyophilized. The resulting cross-linking ODN was analyzed and purified by reverse-phase HPLC using a linear gradient of 5−25% MeCN in 0.1 M TEAA buffer (pH 7.0).

Enzymatic Digestion for Analyses of Nucleoside Composition of ODNs. A mixture of oligodeoxynucleotides (0.2 OD), snake venom phosphodiesterase (MP Biochemicals, 2.0 mg/mL; 6 μL), nuclease P1 (Yamasa Co., 1 unit/μL; 5 μL) and calf intestine alkaline phosphatase (Takara Bio Inc., 0.1 U/mL; 5 μL) in 0.1 M Tris-HCl, 2 mM $MgCl_2$ buffer (pH 7.7) in a total volume of 500 μL was incubated at 37 °C for 12 h. After the reaction mixture was heated at 100 °C for 5 min, the enzymes were filtered off through Micropure-EZ device (Millipore Co.). The filtrate was concentrated to dryness, and the residue was dissolved in H_2O (100 μL) and analyzed by reverse-phase HPLC with a 5−25% MeCN in 0.1 M TEAA buffer (pH 7.0) linear gradient. Nucleoside composition was quantified by dividing each peak area from the HPLC profile, and the results were the following. **dsODN 1**: upper, calcd for dC:dG:T:dA:**2**:**3** = 5:6:4:2:1:1, found 5.9:6.1:3.8:1.8:1.0:1.1; lower, calcd for dC:dG:T:dA:**2**:**3** = 6:5:2:4:1:1, found 6.0:5.2:2.1:3.7:1.0:1.2. **dsODN 2**: upper, calcd for dC:dG:T:dA:**2**:**3** = 5:6:6:2:1:1, found 5.2:6.0:5.8:2.0:1.1:1.0; lower, calcd for dC:dG:T:dA:**2**:**3** = 6:5:4:4:1:1, found 6.3:5.3:4.2:3.7:1.0:1.0. **dsODN 3**: upper, calcd for dC:dG:T:dA:**2**:**3** = 5:6:8:2:1:1, found 5.3:5.9:7.8:2.0:1.2:1.0; lower, calcd for dC:dG:T:dA:**2**:**3** = 6:5:6:4:1:1, found 5.7:5.3:6.2:3.9:0.9:1.2. **tz^{2}ODN 1**: calcd for dC:dG:T:dA:**12** = 11:11:6:6:2, found 11.3:11.2:6.1:5.7:1.9. **tz^{2}ODN 2**: calcd for dC:dG:T:dA:**12** = 11:11:8:6:2, found 11.2:11.3:7.9:5.7:1.9. **tz^{2}ODN 3**: calcd for dC:dG:T:dA:**12** = 11:11:10:6:2, found 10.9:10.8:10.3:5.8:1.9

UV Melting Experiments. Thermally induced transitions were monitored at 260 nm on a Beckman DU 650 spectrophotpmeter. A solution containing 3 μM samples in a buffer of 10 mM sodium cacodylate (pH 7.0) containing 100 mM NaCl was heated at 90 °C for 5 min, then cooled gradually to room temperature and used for the thermal denaturation study. The sample temperature was increased at a rate of 0.5 deg/min.

Labeling of the 5′-Ends of Oligodeoxynucleotides. A mixture of oligodeoxynucleotides (100 pmol), [γ-^{32}P]-ATP (1.7 nmol), and T4 polynucleotide kinase (Takara Bio Inc., 1 U) in a buffer (20 μL) containing Tris-HCl (50 mM, pH 8.0), $MgCl_2$ (10 mM), and DTT (5 mM) was incubated for 45−120 min at 37 °C and heated at 100 °C for 5 min. The resulting solution was purified by column chromatography (C18, YMC dispo SPE, 100 mg/mL) to give 5′-^{32}P-labeled oligodeoxynucleotides.

Determination of Dissociation Constant (K_d) with NF-κB p50 Homodimer by Electromobility Sift Assay. ^{32}P-Labeled oligonucleotide duplexes (40 fmol) and NF-κB p50 homodimer (Promega Co., various concentration: 0, 1, 5, 10, 15, 20, 50, 100 nM) in HEPES buffer (10 mM, pH 7.5) containing $MgCl_2$ (10 mM), LiCl (50 mM), NaCl (100 mM), spermidine (1 mM), BSA (0.2 mg/mL), poly(dI:dC) (1 nM), IGEPAL-CA630 (0.05%), and glycerol (10%) were incubated at 4 °C for 40 min. The mixture was loaded on 8% native polyacrylamide gel (39:1, acrylamide:bisacrylamide), which was pre-cooled and pre-run (120 V, 1 h) at 4 °C. The gel was electrophoresed at 120 V (4 °C) for 40 min, dried under reduced pressure at 80 °C, and imaged on a IP plate (Fuji Film) for 1−5 h. Quantitative measurements of bound and free oligodeoxynucleotides were carried out by image-analyzer (BAS-2500, Fuji Film). The data, which were plotted as a concentration of NF-κB versus binding ratio, were fit to nonlinear regression according to the following equation: $y = B_{max}x/(K_d + x)$.

Competition Assay. ^{32}P-Labeled contODN (40 fmol), NF-κB p50 homodimers (40 fmol), and dumbbell oligodeoxynucleotides (various concentration: 0, 0.2, 1, 2, 4, 10, 20, 40, 200 nM) in HEPES buffer (10 mM, pH 7.5) containing $MgCl_2$ (10 mM), LiCl (50 mM), NaCl (100 mM), spermidine (1 mM), BSA (0.2 mg/mL), poly(dI:dC) (1 nM), IGEPAL-CA630 (0.05%), and glycerol (10%) were incubated at 4 °C for 40 min. The mixture was loaded on 8% native polyacrylamide gel (39:1, acrylamide:bisacrylamide), which was pre-cooled and pre-run (120 V, 1 h) at 4 °C. The gel was electrophoresed at 120 V (4 °C) for 40 min, dried under reduced pressure at 80 °C, and imaged on a IP plate (Fuji Film) for 1−5 h. The data were analyzed in a manner similar to that of the dissociation constants.

Acknowledgment. This work was supported by grants-in-aid for scientific research from the Ministry of Education. We thank Ms. S. Oka (Center for Instrumental Analysis, Hokkaido University) for measurement of the mass spectra.

Supporting Information Available: Experimental procedures and ^{1}H NMR and ^{13}C NMR spectra for **3**−**9, P**, and **Z**. This material is available free of charge via the Internet at http://pubs.acs.org.

JO702459B